Supporting Information for

Calcium Gluconate-Derived Carbon Nanosheet Intrinsically Decorated with Nano-Papillae for Multifunctional Printed Flexible Electronics

*Yiliang Wang, Haomin Wang, Huimin Wang, Mingchao Zhang, Xiaoping Liang, Kailun Xia, and Yingying Zhang**

Key Laboratory of Organic Optoelectronics and Molecular Engineering of the Ministry of Education, Department of Chemistry and Center for Nano and Micro Mechanics, Tsinghua University, Beijing 100084, PR China

Corresponding Author

*E-mail: yingyingzhang@tsinghua.edu.cn.

Figure S1. Photograph of calcium gluconate residues obtained at 400 °C (5 °C/min, N_2).

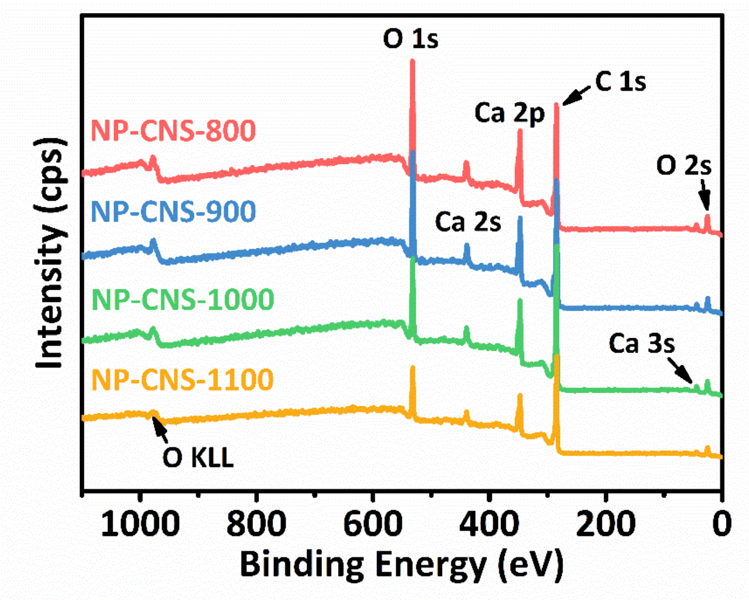

Figure S2. XPS spectra of NP-CNS-800, NP-CNS-900, NP-CNS-1000 and NP-CNS-1100.

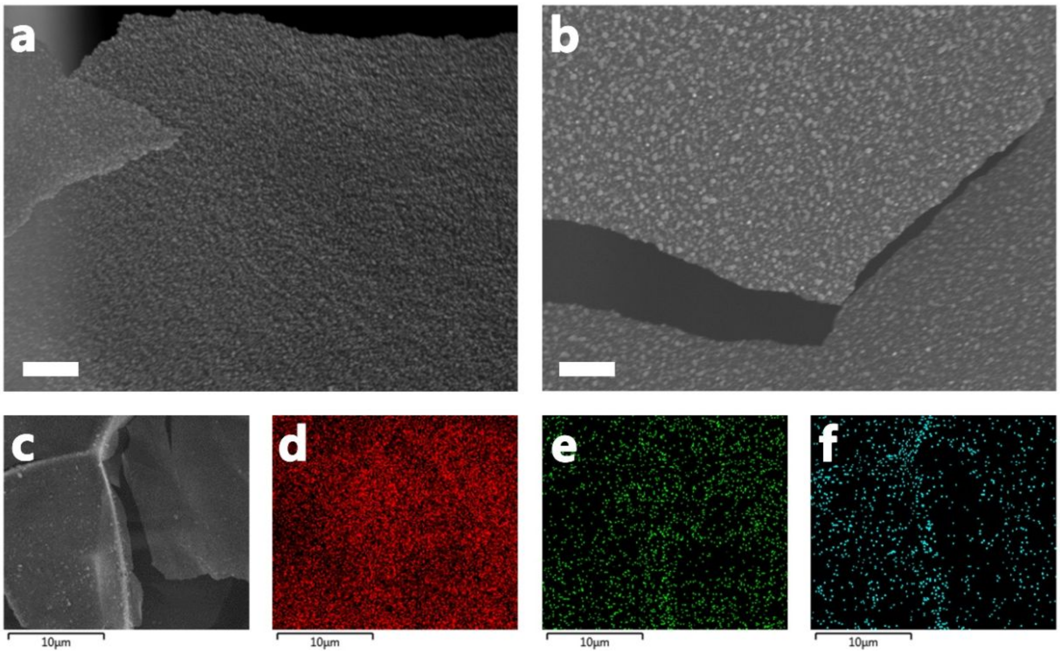

Figure S3. High magnification SEM images and elemental mapping analysis. (a,b) The SEM images of NP-CNS-800 and NP-CNS-1000. (c-f) The SEM image of NP-CNS-1000 (c) and corresponding elemental mapping images C (d), O (e) and Ca (f). Scale bars: (a) 400 nm; (b) 400 nm; (c)-(f) 10 μm.

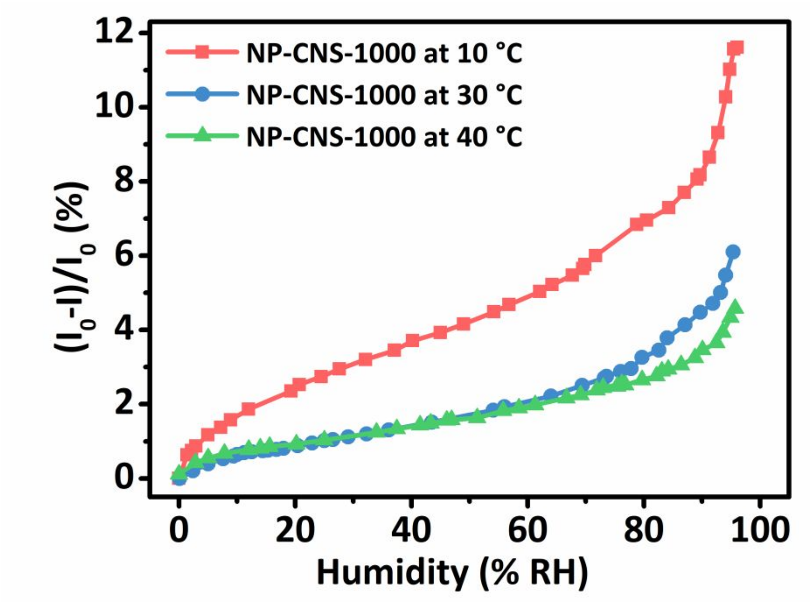

Figure S4. The relative change in current versus humidity applied on the NP-CNS humidity sensor at different temperatures.

Table S1. Summary of main features of flexible printed humidity sensors.

Active material	Working mechanism	Working range (RH)	Response time (s)	Recover time (s)	Ref.
ZnO nanorods	Resistance type	11–95%	5 (11 to 95% RH)	10 (95 to 11% RH)	1
Ag NPs	Capacitance type	30–80%	–	–	2
Ag NPs	Capacitance type	30–90%	356 ± 3	367 ± 4	3
PSSNa*	Capacitance type	10–90%	–	–	4
Ag NPs	Capacitance type	10–70%	24 ± 3	22 ± 4	5
Graphene+methyl-red	Capacitance type	5–95%	0.25 (35–100 % RH)	0.35 (35–100% RH)	6
Ag+PI	Capacitance type	16–90%	20 (35–50% RH)	37.7 (50–35% RH)	7
NP-CNS	**Resistance type**	**0–96%**	**1.7 (10–39% RH)**	**100.1 (39–10% RH)**	**Our work**

*PSSNa: poly(styrene sulfonic acid) sodium salt

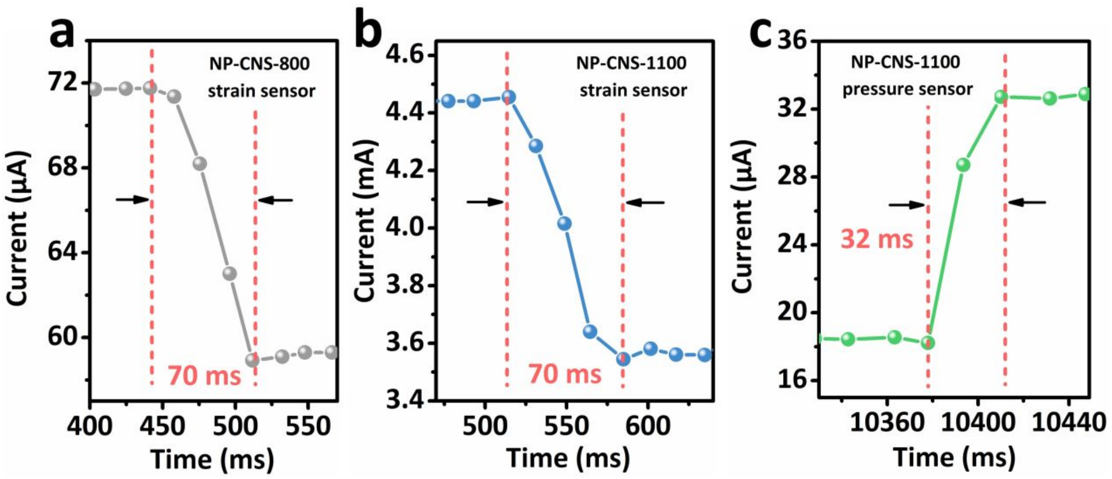

Figure S5. (a) response time of the strain sensor (NP-CNS-800); (b) response time of the strain sensor (NP-CNS-1100); (c) response time of the pressure sensor (NP-CNS-1100).

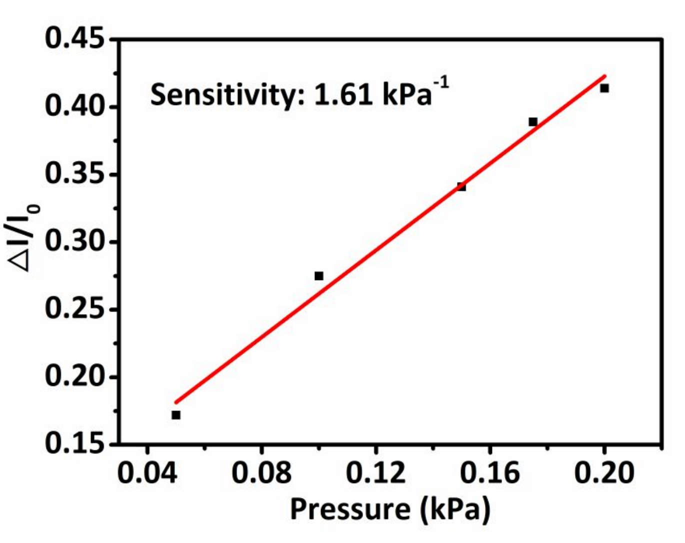

Figure S6. Relative change in resistance of the pressure sensor versus the applied pressure.

Table S2. Summary of main features of flexible resistance-type strain sensors.

Active material	Working range	Sensitivity (GF)	Response time (ms)	Ref.
Ag NWs	<70%	2–14, tunable	≈200	8
Ag NWs	<90%	12 at 5% to 2370 at 70%	–	9
CNT	5–100%	2800 at 5–100%	–	10
CNT	<200%	10.5 at 0–100%	<15	11
Graphene	<70%	0.76 at 10%, 1.67 at 40%, 2.55 at 70%	–	12
rGO	0.2–100%	10 at 1%, 3.7 at 50%	<100	13
Ag NPs	0–450%	35 at 100%, 659 at 150–200%	–	14
Carbonized cotton fabric	>140%	25 at 0–80%, 64 at 80–140%	–	15
MXene+CNT	<130%	64.6 at 0−30%, 772.6 at 40−70%	–	16
CNT	<120%	3350 at 0−110%	–	17
CNT	356%	1.75	–	18
Graphene foam	<70%	3.3–24.1	–	19
Cu NWs	4–420%	1687 at 16−420%	<200	20
NP-CNS	**0–500%**	**21.9 at 0−350%, 99.9 at 350–500%**	**70**	**Our work**

Table S3. Summary of main features of pressure sensors.

Active material	Working mechanism	Low Detection Limit (Pa)	Sensitivity (kPa^{-1})	Response time (s)	Ref.
Carbonized silk nanofiber	Resistance type	–	0.097	≈3	21
CNT	Capacitance type	–	0.7	≈50	22
CNT+graphene	Resistance type	0.6	19.8	<16.7	23
rGO	Resistance type	1.2	15.6	5	24
PEDOT:PSS	Capacitance type	2	0.22	140	25
rGO/polyaniline	Resistance type	–	0.152	96	26
rGO	Resistance type	42	7.94, 178	261	27
NP-CNS	**Resistance type**	**5**	**1.61**	**32**	**Our work**

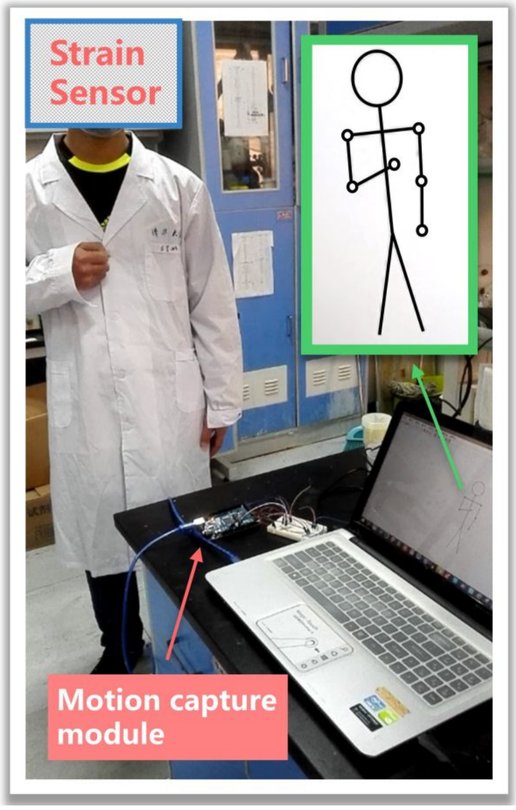

Figure S7. Human motion tracking using NP-CNS-800 sensors and a motion capture module.

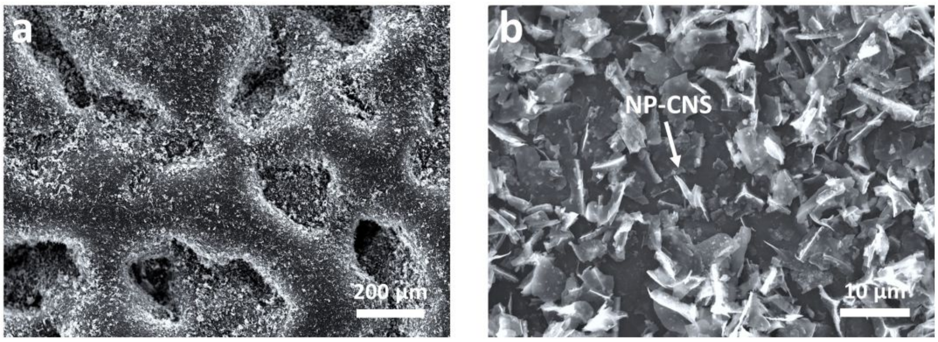

Figure S8. SEM images of the NP-CNS layer in pressure sensor. (a) low-magnification image. (b) high-magnification image.

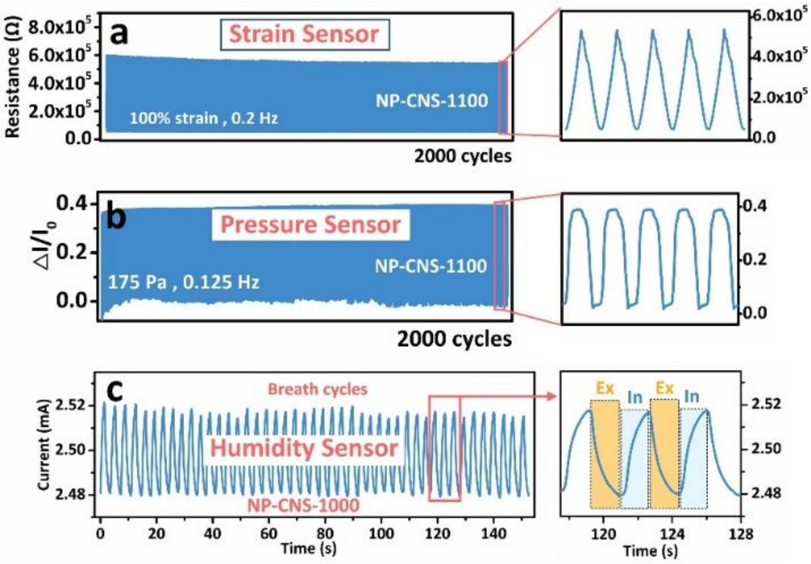

Figure S9. The durability and stability of the humidity, strain, and pressure sensors.

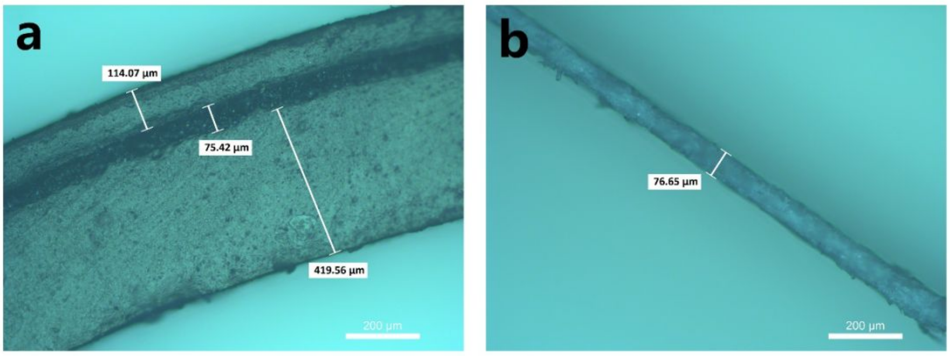

Figure S10. (a) Optical microscope images of the cross section of strain sensor. (b) Optical microscope images of A4 paper.

REFERENCES

1. Qi, Q.; Zhang, T.; Yu, Q.; Wang, R.; Zeng, Y.; Liu, L.; Yang, H. Properties of Humidity Sensing ZnO Nanorods-base Sensor Fabricated by Screen-printing. *Sensors and Actuators B: Chemical* **2008**, 133, 638-643.
2. Reddy, A. S. G.; Narakathu, B. B.; Atashbar, M. Z.; Rebros, M.; Rebrosova, E.; Joyce, M. K. Fully Printed Flexible Humidity Sensor. *Procedia Engineering* **2011**, 25, 120-123.
3. Rivadeneyra, A.; Fernández-Salmerón, J.; Agudo, M.; López-Villanueva, J. A.; Capitan-Vallvey, L. F.; Palma, A. J. Design and Characterization of A Low Thermal Drift Capacitive Humidity Sensor by Inkjet-printing. *Sensors and Actuators B: Chemical* **2014**, 195, 123-131.

4. Wang, X.; Larsson, O.; Platt, D.; Nordlinder, S.; Engquist, I.; Berggren, M.; Crispin, X. An All-printed Wireless Humidity Sensor Label. *Sensors and Actuators B: Chemical* **2012**, 166-167, 556-561.
5. Molina-Lopez, F.; Briand, D.; de Rooij, N. F. All Additive Inkjet Printed Humidity Sensors on Plastic Substrate. *Sensors and Actuators B: Chemical* **2012**, 166-167, 212-222.
6. Ali, S.; Hassan, A.; Hassan, G.; Bae, J.; Lee, C. H. All-printed Humidity Sensor Based on Graphene/methyl-red Composite with High Sensitivity. *Carbon* **2016**, 105, 23-32.
7. Yang, T.; Yu, Y. Z.; Zhu, L. S.; Wu, X.; Wang, X. H.; Zhang, J. Fabrication of Silver Interdigitated Electrodes on Polyimide Films via Surface Modification and Ion-exchange Technique and Its Flexible Humidity Sensor Application. *Sensors and Actuators B: Chemical* **2015**, 208, 327-333.
8. Amjadi, M.; Pichitpajongkit, A.; Lee, S.; Ryu, S.; Park, I. Highly Stretchable and Sensitive Strain Sensor Based on Silver Nanowire–Elastomer Nanocomposite. *ACS Nano* **2014**, 8, 5154-5163.
9. Duan, S.; Wang, Z.; Zhang, L.; Liu, J.; Li, C. A Highly Stretchable, Sensitive, and Transparent Strain Sensor Based on Binary Hybrid Network Consisting of Hierarchical Multiscale Metal Nanowires. *Advanced Materials Technologies* **2018**, 3, 1800020.
10. He, Z.; Zhou, G.; Byun, J. H.; Lee, S. K.; Um, M. K.; Park, B.; Kim, T.; Lee, S. B.; Chou, T. W. Highly Stretchable Multi-walled Carbon Nanotube/thermoplastic Polyurethane Composite Fibers for Ultrasensitive, Wearable Strain Sensors. *Nanoscale* **2019**, 11, 5884-5890.
11. Suzuki, K.; Yataka, K.; Okumiya, Y.; Sakakibara, S.; Sako, K.; Mimura, H.; Inoue, Y. Rapid-Response, Widely Stretchable Sensor of Aligned MWCNT/Elastomer Composites for Human Motion Detection. *ACS Sensors* **2016**, 1, 817-825.
12. Yang, T.; Jiang, X.; Zhong, Y.; Zhao, X.; Lin, S.; Li, J.; Li, X.; Xu, J.; Li, Z.; Zhu, H. A Wearable and Highly Sensitive Graphene Strain Sensor for Precise Home-Based Pulse Wave Monitoring. *ACS Sens* **2017**, 2, 967-974.
13. Cheng, Y.; Wang, R.; Sun, J.; Gao, L. A Stretchable and Highly Sensitive Graphene-Based Fiber for Sensing Tensile Strain, Bending, and Torsion. *Adv Mater* **2015**, 27, 7365-71.
14. Lee, J.; Shin, S.; Lee, S.; Song, J.; Kang, S.; Han, H.; Kim, S.; Kim, S.; Seo, J.; Kim, D.; Lee, T. Highly Sensitive Multifilament Fiber Strain Sensors with Ultrabroad Sensing Range for Textile Electronics. *ACS Nano* **2018**, 12, 4259-4268.
15. Zhang, M.; Wang, C.; Wang, H.; Jian, M.; Hao, X.; Zhang, Y. Carbonized Cotton Fabric for High-Performance Wearable Strain Sensors. *Advanced Functional Materials* **2017**, 27, 1604795.
16. Cai, Y.; Shen, J.; Ge, G.; Zhang, Y.; Jin, W.; Huang, W.; Shao, J.; Yang, J.; Dong, X. Stretchable Ti3C2Tx MXene/Carbon Nanotube Composite Based Strain Sensor with Ultrahigh Sensitivity and Tunable Sensing Range. *ACS Nano* **2018**, 12, 56-62.
17. He, Z.; Byun, J.-H.; Zhou, G.; Park, B.-J.; Kim, T.-H.; Lee, S.-B.; Yi, J.-W.; Um, M.-K.; Chou, T.-W. Effect of MWCNT Sontent on the Mechanical and Strain-sensing Performance of Thermoplastic Polyurethane Composite Fibers. *Carbon* **2019**, 146, 701-708.
18. Wu, X.; Han, Y.; Zhang, X.; Lu, C. Spirally Structured Conductive Composites for Highly Stretchable, Robust Conductors and Sensors. *ACS Appl Mater Interfaces* **2017**, 9, 23007–23016.
19. Zheng, Q.; Liu, X.; Xu, H.; Cheung, M.-S.; Choi, Y.-W.; Huang, H.-C.; Lei, H.-Y.; Shen, X.; Wang, Z.; Wu, Y.; Kim, S. Y.; Kim, J.-K. Sliced Graphene Foam Films for Dual-functional Wearable Strain Sensors and Switches. *Nanoscale Horizons* **2018**, 3, 35-44.
20. Han, S.; Liu, C.; Xu, H.; Yao, D.; Yan, K.; Zheng, H.; Chen, H.-J.; Gui, X.; Chu, S.; Liu, C. Multiscale Nanowire-microfluidic Hybrid Strain Sensors with High Sensitivity and Stretchability. *npj Flexible Electronics* **2018**, 2, 16.

21. Wang, C.; Xia, K.; Zhang, M.; Jian, M.; Zhang, Y. An All-Silk-Derived Dual-Mode E-skin for Simultaneous Temperature-Pressure Detection. *ACS Appl Mater Interfaces* **2017**, 9, 39484-39492.
22. Bae, G. Y.; Han, J. T.; Lee, G.; Lee, S.; Kim, S. W.; Park, S.; Kwon, J.; Jung, S.; Cho, K. Pressure/Temperature Sensing Bimodal Electronic Skin with Stimulus Discriminability and Linear Sensitivity. *Adv Mater* **2018**, e1803388.
23. Jian, M.; Xia, K.; Wang, Q.; Yin, Z.; Wang, H.; Wang, C.; Xie, H.; Zhang, M.; Zhang, Y. Flexible and Highly Sensitive Pressure Sensors Based on Bionic Hierarchical Structures. *Advanced Functional Materials* **2017**, 27, 1606066.
24. Lou, Z.; Chen, S.; Wang, L.; Jiang, K.; Shen, G. An ultra-sensitive and rapid response speed graphene pressure sensors for electronic skin and health monitoring. *Nano Energy* **2016**, 23, 7-14.
25. Kim, H.; Kim, G.; Kim, T.; Lee, S.; Kang, D.; Hwang, M. S.; Chae, Y.; Kang, S.; Lee, H.; Park, H. G.; Shim, W. Transparent, Flexible, Conformal Capacitive Pressure Sensors with Nanoparticles. *Small* **2018**, 14.
26. Ge, G.; Cai, Y.; Dong, Q.; Zhang, Y.; Shao, J.; Huang, W.; Dong, X. A flexible pressure sensor based on rGO/polyaniline wrapped sponge with tunable sensitivity for human motion detection. *Nanoscale* **2018**, 10, 10033-10040.
27. Jia, J.; Huang, G.; Deng, J.; Pan, K. Skin-inspired flexible and high-sensitivity pressure sensors based on rGO films with continuous-gradient wrinkles. *Nanoscale* **2019**, 11, 4258-4266.